Membrane-Bound Electron Transfer Chain of the Thermohalophilic Bacterium *Rhodothermus marinus*: Characterization of the Iron−Sulfur Centers from the Dehydrogenases and Investigation of the High-Potential Iron−Sulfur Protein Function by in Vitro Reconstitution of the Respiratory Chain†

Manuela M. Pereira, João N. Carita, and Miguel Teixeira*

Instituto de Tecnologia Química e Biológica, Universidade Nova de Lisboa, APT 127, 2780 Oeiras, Portugal

Received July 27, 1998; Revised Manuscript Received November 9, 1998

ABSTRACT: *Rhodothermus marinus*, a thermohalophilic bacterium, has a unique electron-transfer chain, containing, besides a cbb_3 and a caa_3 terminal oxidases, a novel cytochrome *bc* complex [Pereira, M. M., Carita, J. N., and Teixeira, M. (1999) *Biochemistry 38*, 1268−1275]. The membrane-bound iron−sulfur centers of this bacterium were studied by electron paramagnetic resonance (EPR) spectroscopy, leading to the identification of its main electron-transfer complexes. The resonances typical for the Rieske-type centers are not detected. Clusters S1 and S3 from succinate dehydrogenase were identified; interestingly, center S3 is shown to be present in two different conformations, with *g* values at 2.035, 2.009, and 2.001 and at 2.025, 2.002, and 2.000. Upon addition of NADH and dithionite, EPR signals assigned to resonances characteristic of binuclear and tetranuclear clusters develop and are attributed to the iron−sulfur centers of complexes I and II. A high-potential iron−sulfur protein- (HiPIP-) type center previously detected in the membranes of this bacterium [Pereira et al. (1994) *FEBS Lett. 352*, 327−330] is shown to belong indeed to a canonical HiPIP. This protein was purified and extensively characterized. It is a small water-soluble protein of ∼10 kDa, containing a single $[4Fe\text{-}4S]^{3+/2+}$ cluster. The reduction potential, determined by EPR redox titrations in intact and detergent-solubilized membranes as well as by cyclic voltammetry in solution, has a pH-independent value of 260 ± 20 mV, in the range 6−9. *In vitro* reconstitution of the *R. marinus* electron-transfer chain shows that the HiPIP plays a fundamental role in the chain, as the electron shuttle between *R. marinus* cytochrome *bc* complex and the caa_3 terminal oxidase, being thus simultaneously identified a HiPIP reductase and a HiPIP oxidase.

Iron−sulfur clusters are the most ubiquitous metal centers in biological systems (*1*). They largely function as one-electron-transfer components in multiple redox chains, although several FeS proteins have specific enzymatic or gene expression regulatory functions (*2*−*5*). In particular, in all the bacterial and archaeal aerobic respiratory chains so far studied, as well as in the mitochondrion, all complexes have at least one iron−sulfur cluster, with the exception of the terminal oxidases.

Iron−sulfur centers differ in their iron content, oxidation state, and reduction potential. According to the iron content, and excluding the simplest mononuclear iron proteins, such as rubredoxins (*6*), three different types of iron−sulfur centers are presently known: [2Fe-2S], [3Fe-4S], and [4Fe-4S]. Under physiologically relevant redox conditions, each of these centers exchanges between only two oxidation states. Complexes I and II (NADH:quinone oxidoreductase and succinate:quinone oxidoreductase) contain $[2Fe\text{-}2S]^{2+/1+}$ centers, with reduction potentials of ∼−250 mV (center N1) and ∼−100/+50 mV (center S1). Complex III (quinol: cytochrome *c* oxidoreductase), commonly designated cytochrome bc_1 complex, contains the Rieske-type [2Fe-2S] cluster, which structurally differs from the other binuclear centers by having one of the iron atoms coordinated to two histidine residues (*7*, *8*); these centers have positive reduction potentials, in the range of +200 to +400 mV. A $[3Fe\text{-}4S]^{1+/0}$ cluster is present only in succinate dehydrogenases (center S3), having reduction potentials between 0 and +50 mV. The tetranuclear clusters of the $[4Fe\text{-}4S]^{2+/1+}$ types also occur in the dehydrogenases, having low reduction potentials, in the range of ∼−350 to −200 mV.

The tetranuclear clusters may function between the 3+ and 2+ states, at a positive reduction potential (between +50 and +450 mV), in the proteins designated high-potential iron−sulfur proteins (HiPIP)[1] (*9*). HiPIPs are small and soluble proteins containing a single tetranuclear cluster, found mainly in purple photosynthetic bacteria (*9*−*11*). Although

† M.M.P. is the recipient of a grant from the PRAXIS XXI program (BD/2758/94). The work was supported by PRAXIS XXI grants, by European Commission Grant CT94-0626, and by European Union G-Project on Biotechnology of Extremophiles (Bio4-CT96-0488).

* Corresponding author: Phone 351-1-4469844; Fax 351-1-4428766; E-mail miguel@itqb.unl.pt.

[1] Abbreviations: HiPIP, high-potential iron−sulfur protein; DM, dodecyl β-D-maltoside; DBMIB, 2,5-dibromo-3-methyl-6-isopropyl-*p*-benzoquinone; SB12, *N*-dodecyl-*N*, *N*-dimethyl-3-ammonio-3-propanesulfonate; EPR, electron paramagnetic resonance; SDH, succinate dehydrogenase.

10.1021/bi981807v CCC: $18.00
Published on Web 01/08/1999

it is one of the best characterized iron−sulfur proteins, discovered more than 30 years ago, its function is still not fully established. In photosynthetic bacteria, it has been shown that HiPIPs are electron donors to the reaction center (*12*−*15*). A HiPIP-type center was found for the first time to be membrane-bound in *Rhodothermus marinus* (*16*). This microorganism is a strictly aerobic and thermohalophilic Gram-negative bacterium, belonging to the heterogeneous group of *Flexibacter*, *Bacteroids*, and *Cytophaga* species (FBC group) and having an optimum growth temperature of 65 °C (*17*, *18*). In this bacterium neither soluble cytochromes nor a Rieske center was detected. Since *R. marinus* is not a photosynthetic organism the HiPIP must have a different function. As preliminary studies showed that the *R. marinus* HiPIP center was reduced by NADH and succinate only in the presence of cyanide, we suggested that this HiPIP-type center could be involved in the electron-transport chain, possibly transferring electrons between a bc_1 complex analogue and a terminal oxidase (*16*). A HiPIP oxidoreductase activity in the membranes of the aerobically grown facultative phototroph *Rhodoferax fermentans* has been reported since (*19*).

To further understand the unusual electron-transfer chain of *R. marinus* and find possible functional substitutes for some of the typical FeS centers absent in this bacterium, a systematic screening of all metal centers in its membranes was performed by EPR and visible spectroscopies. All membrane-bound heme proteins were identified and characterized showing that, in particular, this bacterium contains two terminal oxidases, of the cbb_3 and caa_3 types, a cytochrome *c* (our unpublished data), and a novel cytochrome *bc* complex (*50*). In this paper we report on the characterization of the non-heme iron centers present in *R. marinus* membranes. Particular attention was given to clarify the role of the HiPIP-type center, to establish a function for such a protein in a nonphotosynthetic organism. By use of purified membrane complexes, a direct electron transfer from a quinol oxidizing complex to an oxygen reductase, the cytochrome caa_3, via HiPIP is shown.

EXPERIMENTAL PROCEDURES

Bacterial Strains and Growth Conditions. In this work *R. marinus* type strain, DSM 4253, and a spontaneous nonpigmented mutant, strain PRQ-62B (*20*) were studied. Large scale growth was performed as in ref *50*. A small scale growth (10 L fermentor) was performed in ^{57}Fe enriched Degryse medium. For this purpose 10 mM ^{57}Fe-citrate, prepared from metallic ^{57}Fe, was added to the growth medium instead of ^{56}Fe-citrate. Cells were harvested at the late stationary phase.

Protein Purification: HiPIP. Membrane preparation was done as described in ref *50*. Solubilization was performed with 2% (w/v) of the detergent SB-12. All chromatographic steps were done on Pharmacia HiLoad and LKB HPLC systems, at 4 °C. The purification steps were monitored by visible and EPR spectroscopies and SDS−PAGE. The detergent-solubilized extract was applied to a DEAE-52 Whatman column, in a buffer of 20 mM Tris-HCl, pH 8, and 0.1% SB12 and eluted with a linear gradient of 0−50% 1 M NaCl. The fraction having the HiPIP was applied to a gel-filtration S200 column, with 20 mM Tris-HCl pH 8, 0.1% SB12, and 150 mM NaCl as eluent. The HiPIP-containing fraction was then applied successively to two ion-exchange columns, a Q-Sepharose and a Mono-Q, in a buffer of 20 mM Tris-HCl, pH 8, and 0.1% SB12 and eluted with linear gradients of 0−50% 1 M NaCl. The HiPIP-type protein was also found, although in almost undetectable amounts, in the soluble fractions. Thus this fraction was applied to a DEAE fast-flow column equilibrated with 20 mM Tris-HCl, pH 8, and eluted with a linear gradient of 0−50% NaCl. The fraction containing the HiPIP (eluted at ∼300 mM NaCl) was loaded onto a gel-filtration Superdex 75 column with 20 mM Tris-HCl, pH 8, and 150 mM NaCl as eluent, and then it was applied to a Mono-Q column. It was eluted in a linear gradient of 0−50% 1 M NaCl, with 20 mM Tris-HCl, pH 8, as buffer. The HiPIP obtained from either the membrane or the soluble fractions, after the Mono-Q steps, was judged to be pure by both SDS−PAGE and visible spectroscopy.

Cytochrome bc and Terminal Oxidases. The cytochrome *bc* complex was purified as in ref *50*. The purification and characterization of the oxidases will be published elsewhere. During the purification of the heme complexes a partially purified fraction containing succinate dehydrogenase was obtained. This fraction comes out of the Q-Sepharose column that separates the cbb_3 oxidase from the cytochrome *bc* complex (*50*).

Molecular Mass. Molecular mass was determined by SDS−15% PAGE performed in a Laemmli discontinuous buffer system (*21*) and HPLC gel-filtration chromatography. Isoelectric points were obtained by use of a Pharmacia IEF Kit.

Amino Acid Sequence. The N-terminal sequence of the HiPIP was determined by the method of Edman and Begg (*22*), with an Applied Biosystem Model 477A protein sequencer.

Protein and Iron Quantification. Protein concentration was determined by the microbiuret method (*23*). The iron content was determined chemically by the 2,4,6-tripyridyl-1,3,5-triazine method (*24*).

Spectroscopic Techniques. Visible spectra were obtained on a Beckman DU-70 or an Olis DW2 spectrophotometer, equipped with a temperature controller. For the thermal stability studies, visible spectra were recorded, after 30 min of incubation at each temperature, under anaerobic conditions. The stability was determined by following the absorption change at 410 nm. EPR spectra were measured as in ref *50*.

Electrochemical Measurements. Cyclic voltammetry experiments were performed as in ref *25* with a pyrolytic graphite-edge electrode (Carbon Loraine). Anaerobic potentiometric titrations were followed by EPR spectroscopy as in ref *26*, with the same redox mediators as in ref *50* but at a final concentration of 20 μM. For the pH variation studies, 200 mM MES−Bis-tris propane was used as buffer at defined pH values from 6 to 9. Reduction potentials are quoted in relation to the standard hydrogen electrode.

Catalytic Activity Assays. Oxygen consumption was measured polarographically at 40 °C, with a Clark-type oxygen electrode, YSI Model 5300, Yellow Springs, OH. Menadiol:HiPIP oxidoreductase and HiPIP oxidase activities were measured by monitoring the change in absorbance of HiPIP at 480 nm ($\Delta\epsilon_{480}$ = 10 000 M^{-1} cm^{-1}), at room

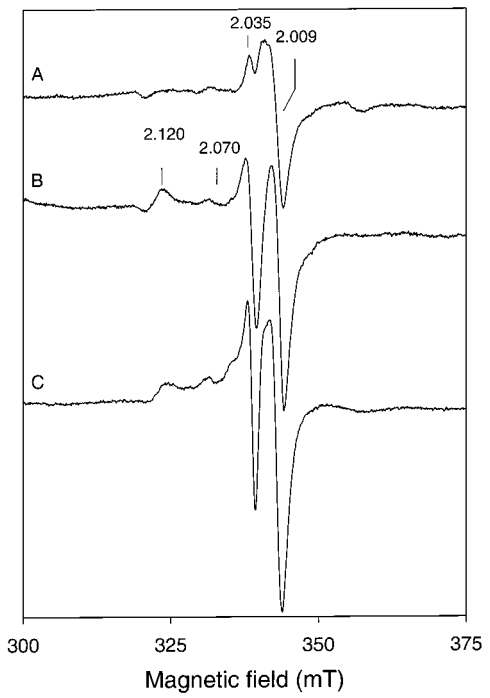

FIGURE 1: EPR spectra of *R. marinus* cells as recovered (A), ferricyanide-oxidized cells (B), and membranes (C) at 10 K. Microwave frequency, 9.64 GHz; microwave power, 2.4 mW; modulation amplitude, 0.9 mT.

temperature. Menadiol was prepared as described in ref *27*. All assays were carried out with 20 mM Tris-HCl, pH 8, and 0.1% DM as buffer.

RESULTS

The usual catalytic activities involved in oxygen-utilizing electron transport chains are present in *R. marinus* membranes. These activities were measured polarographically at 40 °C and respiratory rates of 10, 7.5, and 1.5 nmol of O_2 min^{-1} (mg of protein)$^{-1}$ were obtained for TMPD, NADH, and succinate oxidase activities, respectively. These activities are most probably underestimated, since the bacterium has an optimum growth temperature of 65 °C. Both succinate and NADH fully reduce all the heme centers present in *R. marinus* membranes, as indicated by visible spectra of solubilized membranes incubated anaerobically with these substrates, in the presence of cyanide. Classical inhibitors of complex III, such as DBMIB, antimycin A, and myxothiazol, had no inhibitory effect on the respiration rates.

R. marinus Oxidized Membranes. The EPR spectrum of *R. marinus* cells, as recovered, is dominated by intense resonances at $g \sim 2.03$ and ~2.0 (Figure 1, spectrum A), which were deconvoluted into two components with $g =$ 2.035, 2.009, and 2.001 and $g = 2.025$, 2.002, and 2.000 (see below). Minor signals due to Mn(II) at both higher and lower magnetic field are also observed. Upon oxidation with addition of ferricyanide, those resonances persist and strong resonances at $g = 2.120$, 2.070, and 2.030 develop (Figure 1, spectrum B), due to the HiPIP-type center (*16*; see also below).

R. marinus membranes as isolated exhibit an EPR spectrum almost identical to that of oxidized cells (Figure 1, spectrum C). The intensity of these resonances did not increase by addition of excess potassium ferricyanide or potassium persulfate, in either intact or solubilized membranes. The soluble fraction, apart from a sharp resonance due to a trinuclear [3Fe-4S] cluster of a ferredoxin (our unpublished data), does not show any other signals, even upon oxidation with excess ferricyanide, indicating that the HiPIP center is strongly attached to the membranes.

The paramagnetic metal centers present in the oxidized membranes were deconvoluted upon reduction with different electron donors. Upon addition of hydroquinone [$E' = 285$ mV (*28*)], the HiPIP is reduced, with a persisting set of resonances almost identical to those observed in the cells, in agreement with the previously determined redox midpoint potential (*16*) (Figure 2A, spectrum a).

Addition of substoichiometric amounts of menadiol leads also to full reduction of the HiPIP (Figure 2A, spectra b and c); however, the actual spectra obtained in the $g \sim 2$ region differ as to the relative proportion of the $g = 2.035$ and $g =$ 2.025 species. These resonances were clearly identified as the same observed in the intact cells, and further addition of either menadiol or ascorbate leads to their complete bleaching. These signals are optimally detected at around 10 K and observed up to ~15 K, above which temperature they start broadening beyond detection due to increase in the electronic relaxation. The resonances are slightly broader in membranes from ^{57}Fe-enriched samples, showing an increase of ~1 mT in line width as deduced both from direct measurement of the peak-to-peak width and by theoretical simulation (data not shown). The two species were further characterized by comparison with the spectra from the partially purified fraction containing succinate dehydrogenase, which shows these resonances. Taking advantage of the different proportions accidentally obtained for these species, it was possible to perform their deconvolution and simulation (Figure 2B, Table 1): one species has g values at 2.035, 2.009, and 2.001 and the other at 2.025, 2.002, and 2.000. The signals were integrated to a 1:1 ratio in the SDH fraction, as well as in the cells and in the membranes. The use of glycerol, as a glassing agent, causes a change in the line width and g values of the signal with $g_{max} = 2.025$, while the first signal is essentially unaltered (Figure 2B, spectrum e), but the same stoichiometry is obtained. In the partially purified fraction the reduction of these centers shows in parallel-mode EPR a signal typical of reduced [3Fe-4S] clusters, at $g \sim 12$ (data not shown).

The membrane suspension was titrated, monitoring the intensities of the EPR resonances at $g \sim 2.03$ and of the HiPIP. While it was possible to achieve redox equilibration with the HiPIP center, which allowed us to redetermine its reduction potential in the membrane-bound form at a wide pH range (6−9), the centers at $g \sim 2.03$ proved difficult to follow, due both to superposition with the HiPIP and mediator radical signals, as well as to bad equilibration. Hence, only an upper limit of ~200 mV could be determined for their reduction potentials. However, using the SDH-containing fraction, both species titrate following a Nernst curve ($n = 1$), with a reduction potential of $+135 \pm 10$ mV (data not shown). Along the titration the line shape and stoichiometry of the two signals did not change.

Another paramagnetic center is present in the oxidized state, associated with the cytochrome *bc* complex (*50*). However, due to its very fast relaxation, it is only well observed at 4.7 K, being barely detected at 10 K.

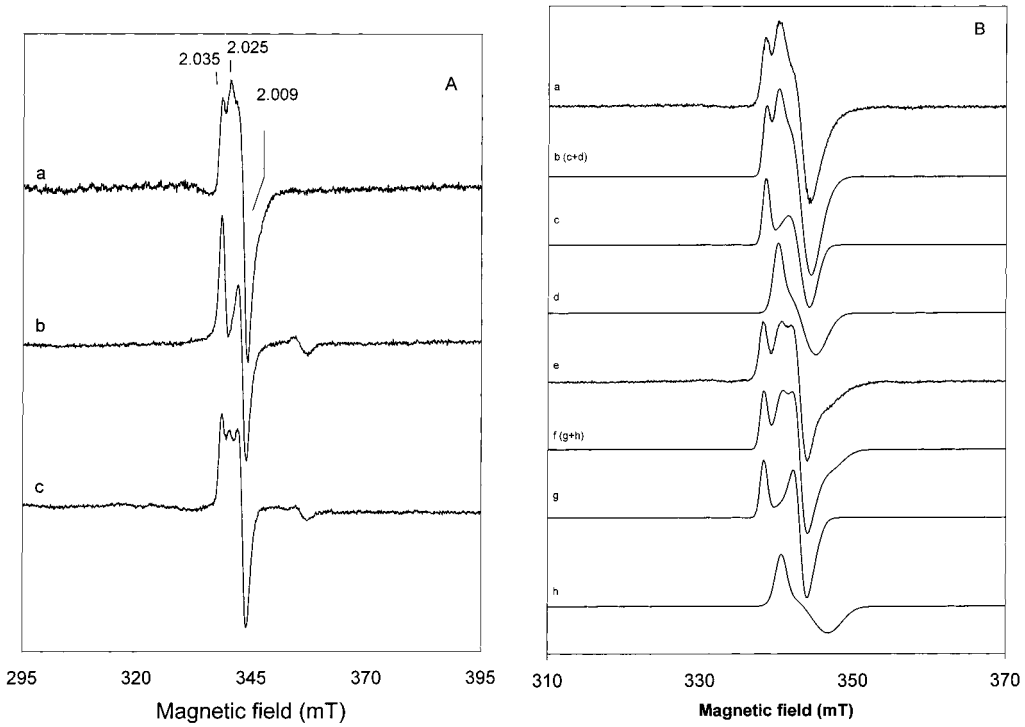

FIGURE 2: (A) EPR spectra of *R. marinus* membranes reduced with hydroquinone (a) and menadiol (b, c). (B) EPR spectra of *R. marinus* partially purified succinate dehydrogenase-containing fraction in the oxidized state, in the absence (a) or presence (e) of glycerol, simulation of the total spectra (b and f) with parameters in Table 1, and deconvolution of the different components (c, d, g, and h). Simulations were calculated with the following g values: $g_{max,med,min} = 2.035, 2.009, 2.001$ (spectra c and g) and $g_{max,med,min} = 2.025, 2.002, 2.000$ (spectra d and h). Experimental spectra were obtained at 10 K. Microwave frequency, 9.64 GHz; microwave power, 2.4 mW; modulation amplitude, 0.9 mT.

Table 1: EPR g Values and Reduction Potentials at pH 7 for *R. marinus* Iron−Sulfur Centers

	center	E' (mV)	g_{max}	g_{med}	g_{min}
complex I	N1 (?)	nd[a]	2.025	1.933	1.933
	N2 (?)	nd	2.030	1.939	1.926
	N3	nd	2.020	1.940	1.865
	N4	nd	2.065	1.940	1.898
complex II	S1	nd	2.030	1.939	1.926
	S3a	135	2.025	2.002	2.000
	S3b	135	2.035	2.009	2.001
HiPIPa		260[b]	2.120	2.030	2.030
HiPIPb			2.120	2.070	2.030

[a] nd, not determined. [b] Reduction potential pH independent in the range 6−9.

The HiPIP, $g = 2.035$, and $g = 2.025$ species account for all the paramagnetic centers observed in the oxidized membranes. The EPR spectrum of the membranes was fully reproduced (Figure 3) by using a stoichiometry of 4:1:1 for the HiPIP and the species at $g = 2.035$ and $g = 2.025$, respectively.

R. marinus Reduced Membranes. Incubating *R. marinus* membranes with sodium succinate (∼30 mM), in the presence of cyanide, leads to almost full bleaching of the EPR resonances at $g \sim 2$ and development of a quasi-axial signal with g values of 2.030 and 1.939 (Figure 4). The same species is observed in the SDH-containing fraction, reduced with succinate or sodium dithionite, enabling its assignment to SDH center S1 (*29*−*32*). Particularly well observed at 20 K and observable up to ∼70 K without noticeable broadening, this resonance is remarkably similar to that of *Escherichia coli* SDH (*29*−*31*). Both by manual double integration of the experimental spectra of this fraction obtained under nonsaturating conditions and from the respective theoretical simulations (Table 1), it was found that together the $g = 2.035$ and 2.025 species quantitate for one center, S1.

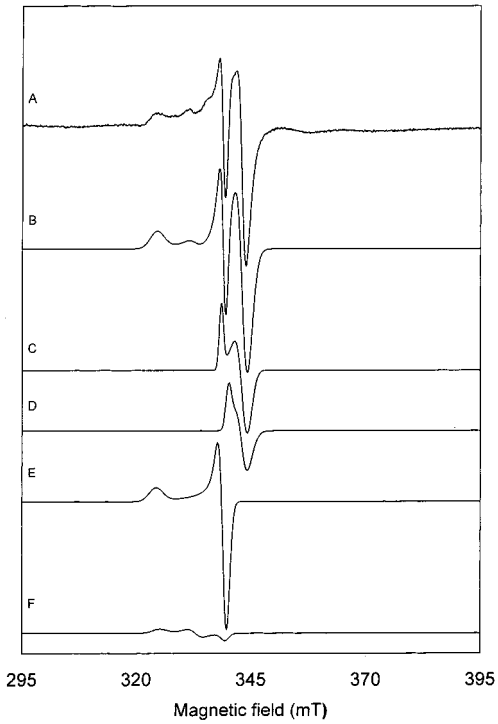

FIGURE 3: EPR spectrum of *R. marinus* oxidized membranes at 10 K (A), simulation of the total spectrum (B), and simulations of the different components: S3a (C), S3b (D) and HiPIPa and HiPIPb (E and F), with parameters in Table 1. Microwave frequency, 9.64 GHz; microwave power, 2.4 mW; modulation amplitude, 0.9 mT.

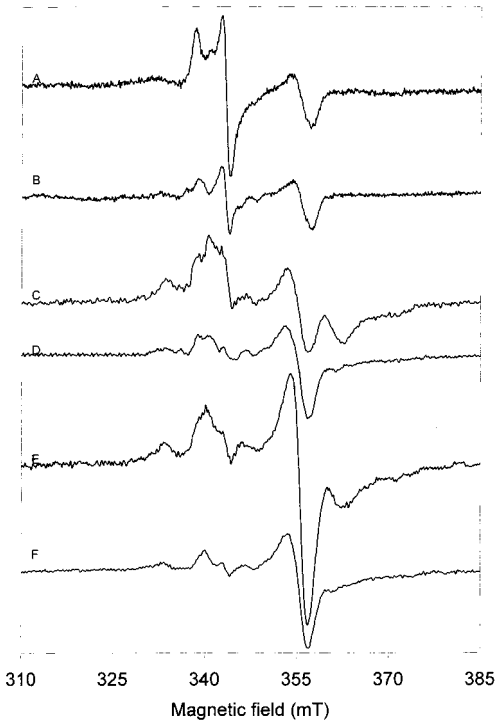

FIGURE 4: EPR spectra of *R. marinus* reduced membranes with sodium succinate (A, B), NADH (C, D), and dithionite (E, F) in the presence of cyanide. Temperatures were 10 K (A, C, and E) and 20 K (B, D, and F). Microwave frequency, 9.64 GHz; microwave power, 2.4 mW; modulation amplitude, 0.9 mT.

Upon reduction of the membranes with 10 mM NADH, also in the presence of cyanide, the resonances around $g \sim 2$ disappear and several signals at $g = 2.065$, 2.02, 1.940, 1.898, and 1.865 are observed at 10 K (Figure 4, spectrum C). At 20 K the spectrum is considerably simplified, being dominated by a quasi-axial signal with g values of 2.025 and 1.933 (Figure 4, spectrum D). Addition of sodium dithionite increases the intensity of the resonances at 1.933, at 10 K, but at higher temperature only a slight increase in intensity is observed (Figure 4, spectra F and G). The spectra thus obtained were tentatively analyzed by comparison with the clusters observed in NADH dehydrogenases (*33*, *34*). Resonances very similar to those assigned to the tetranuclear clusters N3 and N4 of *E. coli* (*34*) and *Neurospora crassa* (*33*) NADH dehydrogenase are clearly observed, in a 1:1 ratio. The other centers are difficult to assign, due to the superposition of center S1 and to the lack of a clear effect by rotenone. However, the differences observed upon NADH and dithionite reductions at 10 and 20 K indicate that at least one center similar to clusters N1 and N2 could be present. Use of redox mediators, such as methyl viologen and benzyl viologen, did not cause any significant change in the relative spectral intensities. Hence it becomes unclear whether centers equivalent to N1 and N2 are present in *R. marinus*. As previously reported (*16*), no Rieske-type resonances were observed upon reduction with hydroquinone, menadiol, or any other electron donor used.

R. marinus HiPIP. As described in ref *50*, prior to solubilization, the membrane fraction was successively washed with low and high ionic strength buffers. The resultant supernatants did not contain HiPIP, as judged by the absence of the characteristic resonances in their EPR spectra, confirming our previous observation that this protein is strongly attached to the membranes (*16*). Only a very minor amount of HiPIP could be detected in the soluble fractions.

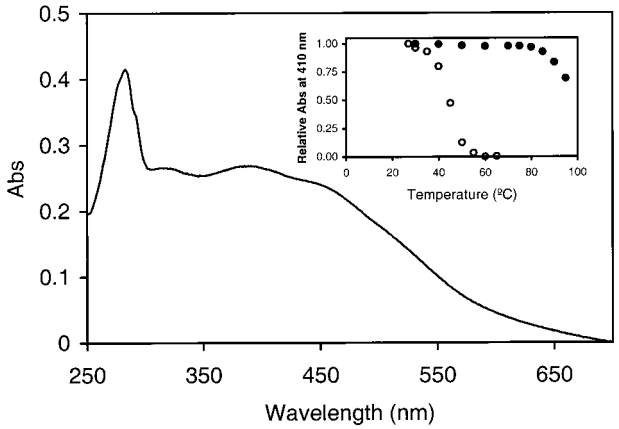

FIGURE 5: Visible spectrum of *R. marinus* oxidized HiPIP. (Inset) Thermostability profiles for *R. marinus* (●) and *Ectothiorhodospira halophila* (○) HiPIPs.

The HiPIP-type center containing protein was now fully purified to homogeneity as judged by SDS−PAGE, which reveals a single band, and by the purity index (see below). The proteins obtained from either the membranes or the soluble fraction are identical and, as described below, have all the characteristics of a HiPIP. Upon detergent removal, the HiPIP purified from the membranes is water-soluble. This HiPIP is a monomer with a molecular mass of 10.5 kDa, as estimated from SDS−PAGE and gel filtration. It has an isoelectric point of 5.5 and contains four iron atoms per molecule. The N-terminal sequence of *R. marinus* HiPIP is AELTXTDVSGLTPEEIQMRESLQ**Y**TDHSPYPDKTA. HiPIPs show a very low amino acid sequence homology (*35*, *36*). The same is observed for the *R. marinus* HiPIP—no conserved residues are observed apart from a tyrosine in position 24, which is located near the tetranuclear cluster and is most probably structurally important (*37*).

The visible spectrum, in the oxidized form, has a maximum at 283 nm and broad bands at 316, 380, and 450 nm (Figure 5). The purity index of the oxidized state ($A_{280}/A_{380} = 1.5$) is well within the range published for other HiPIPs (*38*), further confirming its purity. Upon reduction a 40% decrease in the absorbance in the region of 400−500 nm occurs. As expected from a protein isolated from a thermophile, *R. marinus* HiPIP is very thermostable: the visible spectrum remains unaltered up to 80 °C, in contrast with the HiPIP isolated from the mesophilic bacterium *Ectothiorhodospira halophila* (inset, Figure 5). The EPR spectrum of the purified HiPIP is similar to that observed in the membranes. It is quasi-axial, with g values at 2.120 and 2.030. A rhombic component is also observed, with g values at 2.130, 2.070, and 2.030 (Figure 6), which contributes 10% to the total spectrum. The origin of this component, observed in almost all HiPIPs, remains unclear, and it has been suggested that it may correspond to a different electronic distribution among the irons of the cluster (*39*).

The reduction potential of the purified HiPIP was determined by cyclic voltammetry, at pH 7. A direct, unmediated, and reversible response was obtained, from which a reduction potential of 290 ± 10 mV was determined, a value very close to that measured from the redox titrations of intact mem-

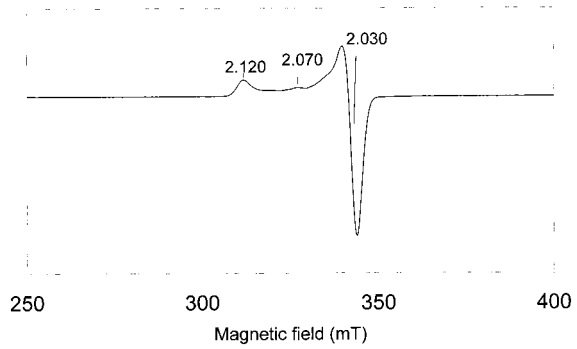

FIGURE 6: EPR spectrum of *R. marinus* HiPIP, at 10 K. Experimental conditions were as in Figure 1.

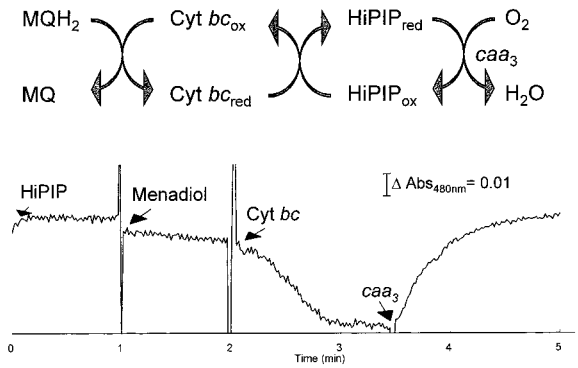

FIGURE 7: (A) Schematic representation of *R. marinus* electron-transfer chain from menaquinol to oxygen. (B) Spectrophotometric assay following the HiPIP change in absorbance at 480 nm upon successive additions of menadiol (1 mM), cytochrome *bc* complex (0.3 μM), and *caa*$_3$ oxidase (0.05 μM).

branes in the pH range 6−9 (data not shown). The minor component with $g = 2.07$ titrates together with the major EPR species.

HiPIP Function. It was observed previously that in the membranes the HiPIP was reduced upon addition of succinate or NADH, in the presence of cyanide (*16*). By use of the purified HiPIP and heme complexes from *R. marinus*, its function could be now clearly established. By EPR spectroscopy, it is observed that upon addition of catalytic amounts of cytochrome *bc* complex to a sample containing the HiPIP and menadiol, the iron−sulfur protein is fully reduced, showing that the HiPIP acts as an electron acceptor of the cytochrome *bc* complex. A more complete experiment was performed (Figure 7), by use of visible spectroscopy: following the change in absorbance of the HiPIP at 480 nm, in a reaction mixture containing the HiPIP (7 μM), when menadiol is added (1 mM) practically no reduction is observed. Addition of substoichiometric amounts of cytochrome *bc* complex (0.3 μM) leads to HiPIP reduction, as expected from the EPR results; when the *caa*$_3$ terminal oxidase is added (0.05 μM) a complete reoxidation of the HiPIP is observed. Addition of potassium cyanide, which inhibits the oxidase, leads to the rereduction of the HiPIP (data not shown). This experiment clearly shows that HiPIP functions by transferring electrons between the cytochrome *bc* complex and the terminal oxidase, coupling the oxidation of menadiol to the reduction of oxygen according to the scheme represented in Figure 7. A turnover of 208 min^{-1} was determined, at room temperature for the oxidation of HiPIP by the *caa*$_3$ oxidase, a value much higher than that obtained for the monohemic cytochrome from *R. marinus* (16 min^{-1}) or for horse heart cytochrome (45 min^{-1}) and comparable to that determined for TMPD oxidation (250 min^{-1}) (our unpublished data). For the reduction of the HiPIP by the cytochrome *bc* the turnover is double that determined with the horse heart cytochrome (40 min^{-1} versus 22 min^{-1}). It should be stressed, however, that these numbers are most probably underestimated, mainly because the measurements were done at room temperature, quite far from the optimal growth temperature of *R. marinus* (65 °C). A similar experiment was performed with the *cbb*$_3$-type oxidase. Oxidation of the HiPIP was also observed upon addition of this oxidase. However, it became rapidly rereduced, suggesting that under the experimental conditions the coupling of menadiol oxidation, by the cytochrome *bc* complex, to oxygen reduction, by the *cbb*$_3$ oxidase, via the HiPIP is not efficient.

DISCUSSION

In this paper the iron−sulfur centers present in *R. marinus* membranes were identified. It was shown that the previously detected HiPIP-type center belongs to a small HiPIP, which is firmly attached to the membrane. This attachment is most probably established through a strong electrostatic interaction with other protein complexes. In agreement with our previous observations (*16*), no Rieske-type protein was detected by EPR spectroscopy either in intact membranes or in any soluble or membrane fractions. This membrane-bound HiPIP was proved to be the electron carrier between the *R. marinus* menaquinol-oxidizing *bc* complex and the *caa*$_3$ oxidase (see also below).

Paramagnetic species analogous to those of centers S1 and S3 from succinate dehydrogenases were observed in the membranes and in a partially purified fraction. Due to its relaxation properties (*30*) it is not possible to observe center S2 in membrane preparations, which is overlaid by the resonances of complex I. The EPR signal with g_{max} at 2.025 is very similar to that of the trinuclear centers (*40*−*42*). As it is reduced by succinate in the membranes, in the presence of cyanide, as well as in the partially purified SDH-containing fraction, it is assigned to center S3 of this complex. Similarly, the axial species observed upon reduction, with $g = 2.03$ and 1.93, is assigned to center S1.

The center with g_{max} at 2.035 in the oxidized state could not be separated from S3. They are both reduced by succinate, have the same reduction potential, and are present in equal amounts. Also, the two species show similar line broadening in the EPR spectra of ^{57}Fe-enriched membranes. Moreover, the sum of their intensities quantitates to an amount equivalent to center S1. All these data strongly suggest that it corresponds to an alternative conformation of center S3. Interestingly, EPR signals with g_{max} at ∼2.03 and 2.00 have been previously observed in inactive forms of some soluble enzymes, such as aconitases, L-serine hydratase, and endonuclease III (*43*−*46*). They were unequivocally attributed to trinuclear centers, resulting from the oxidative damage of [4Fe-4S] clusters. However, in the case of *R. marinus* this seems not to be the case since that species is already observed in intact cells, is stable under oxygen (as expected for an aerobic bacterium), and is physiologically active in the oxygen-utilizing electron-transfer chain. The reason for this apparent heterogeneity

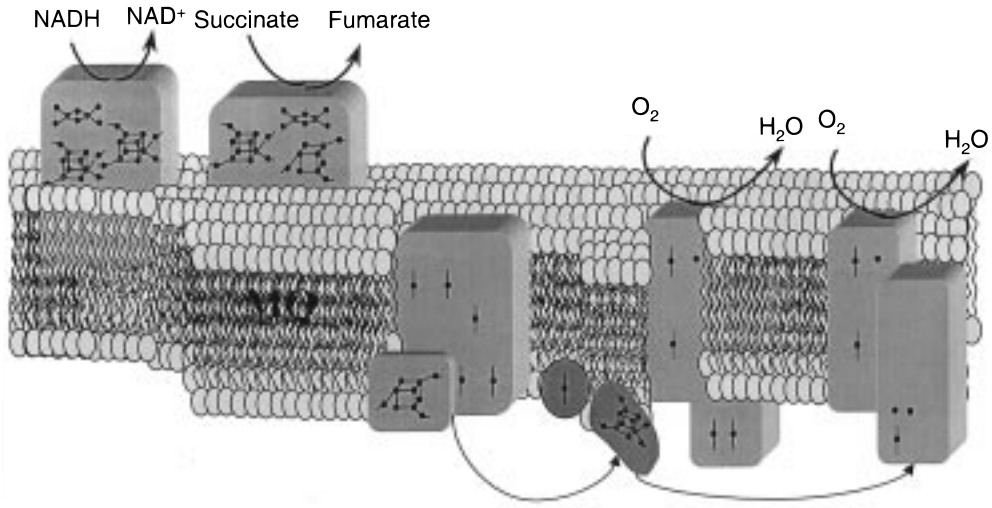

FIGURE 8: Schematic representation of *R. marinus* electron transport chain. This contains an NADH and succinate dehydrogenases, two terminal oxidases of the caa_3 and cbb_3 types and a novel cytochrome *bc* complex analogue to the mitochondrial complex III [accompanying paper (*50*) and our own unpublished data]. The electron carriers are menaquinone, the HiPIP, and *R. marinus* cytochrome *c* [accompanying paper (*50*) and our own unpublished data]. All metal centers were represented without implying any spatial arrangement.

remains to be understood, but interestingly the effect of glycerol was also observed for the inactive form of aconitase A from *E. coli*. In the absence of the glassing agent the EPR spectrum of this enzyme resembles that with g_{max} at 2.025, but with glycerol the spectrum becomes similar to that with g_{max} at 2.035 (*42*), suggesting that a minor conformational change is responsible for the spectral modifications observed. Moreover, such an effect was also reported to occur in L-serine dehydratase from *Peptostretococcus asaccharolyticus* by changing buffers (*45*). Since 3Fe centers have been proposed to interact with the quinones (*47*) experiments were performed by incubating the succinate dehydrogenase fraction with menadione and menadiol; however, no change of the relative proportion of the two species was observed.

The reduction of the membranes with NADH led to the identification of several species assigned to the iron−sulfur clusters N3 and N4 of type I NADH dehydrogenase (e.g., ref *31*); clear evidence for the presence of clusters N1 and N2 could not be obtained at this stage. Although at the present stage a complete identification of the centers associated with succinate and NADH dehydrogenases was not possible, it becomes nevertheless clear that *R. marinus* contains complexes I and II similar to those of mesophilic bacteria and mitochondria.

The data gathered on the *R. marinus* respiratory chain is presented schematically in Figure 8. This bacterium contains analogues of complexes I and II, which reduce menaquinone, the main quinone present in its membranes (*48*). All heme centers are reduced upon addition of NADH or succinate, in the presence of cyanide, indicating that they are all associated with the respiratory chain, in agreement with the reduction potentials determined (*50*; our unpublished data). No typical bc_1 complex is present, but a functional analogue was found (*50*): it is a multihemic *bc* complex with menadiol:HiPIP oxidoreductase activity. A cytochrome *c* with a reduction potential identical to that of the HiPIP is also present in *R. marinus*, although in very small amounts (our unpublished data). No small and soluble electron carriers, such as copper or Rieske-type proteins or cytochromes *c*, were found. The HiPIP and *R. marinus* cytochrome *c* are the ultimate electron donors for the caa_3 terminal oxidase, functioning as an analogue of the mitochondrial cytochrome. It is noteworthy that HiPIP is a much better electron donor to this oxidase than horse heart or *R. marinus* cytochrome *c*, as evidenced by the respective turnovers.

In conclusion, we have now established the function for a HiPIP, as the electron carrier between the novel cytochrome *bc* complex (complex III in the *R. marinus* respiratory chain) and the terminal caa_3 oxidase. Simultaneously, a new type of electron donor, an iron−sulfur protein, for a so far considered cytochrome oxidase was also identified. The finding of a novel quinol-oxidizing complex (*50*) and the involvement of an iron−sulfur protein as the ultimate electron donor to a terminal oxidase opens new views on oxygen-reducing electron-transfer chains, not only showing an unexpected diversity of its basic components but also enabling us to highlight which are indeed the essential components of these chains. The HiPIP is added now to the increasing list of electron donors to oxygen reductases, which comprises the various types of monohemic cytochromes, quinols, and possibly the putative mononuclear copper proteins, such as sulfocyanin (*49*).

ACKNOWLEDGMENT

We thank the IBET fermentation plant for the bacterial growth, Professor Olle Holst, Lund University, for the kind gift of *R. marinus* cells, and Manuela Regalla (ITQB) for performing the N-terminal sequence. We are grateful to Professor António Xavier and Robert Anglin for the critical reading of the manuscript. *R. marinus* strains were given by Professor M. da Costa.

REFERENCES

1. Cammack, R. (1992) *Advances in Inorganic Chemistry, Iron−Sulfur Proteins*, Vol. 38, Academic Press, San Diego, CA.
2. Beinert, H., and Thomson, A. J. (1983) *Arch. Biochem. Biophys. 222*, 333−361.

3. Bates, D. M., Lazazzera, B. A., and Kiley, P. J. (1995) *J. Bacteriol. 177*, 3972−3978.
4. Melville, S. B., and Gunsalus, R. P. (1996) *Proc. Natl. Acad. Sci. U.S.A. 93*, 1226−1231.
5. Rouault, T. A., and Klausner, R. D. (1996) *Trends Microbiol. Lett. 21*, 174−177.
6. Sieker, L. C., Stenkamp, R. E., and LeGall, J. (1994) in *Methods in Enzymology* (Peck, H. D., and LeGall, J., Eds.) Vol. 243, pp 203−216, Academic Press, San Diego, CA.
7. Iwata, S., Saynovits, M., Link, T. A., and Michel, H. (1996) *Structure 4*, 567.
8. Xia, D., Yu, C.-A., Kim, H., Xia, J.-Z., Kachurin, A. M., Zhang, L., Yu, L., and Deisenhofer (1997) *Science 277*, 60−66.
9. Bartsch, R. G. (1991) *Biochim. Biophys. Acta 1058*, 28−30.
10. Meyer, T. E., Prezysiecki, C. T., Watkins, J. A., Bhattacharyya, A., Simondsen, R. P., Cusanovich, M. A., and Tollin, G. (1983) *Proc. Natl. Acad. Sci. U.S.A. 80*, 6740−6744.
11. Meyer, T. E. (1994) *Methods Enzymol. 243*, 435−448.
12. Meyer, T. E., Bartsch, R. G., Cusanovich, M. A., and Tollin, G. (1993) *Biochemistry 32*, 4719−4726.
13. Hochoeppler, A., Ciurli, S., Venturoli, G., and Zannoni, D. (1995) *FEBS Lett. 357*, 70−74.
14. Shoepp, B., Parot, P., Menin, L., Gaillard, J., Richaud, and Verméglio, A. (1995) *Biochemistry 34*, 11736−11742.
15. Hochoeppler, A., Zannoni, D., Ciurli, S., Meyer, T. E., Cusanovich, M. A., and Tollin, G. (1996) *Proc. Natl. Acad. Sci. U.S.A. 93*, 6998−7002.
16. Pereira, M. M., Antunes, A. M., Nunes, O. C., Costa, M. S., and Teixeira, M. (1994) *FEBS Lett. 352*, 327−330.
17. Alfredsson, G. A., Kristjansson, J. K., Hjörleifsdottir, S., and Stetter, K. (1988) *J. Gen. Microbiol. 134*, 299−306.
18. Andrésson, O. S., and Fridjónsson, O. H. (1994) *J. Bacteriol. 176*, 6165−6169.
19. Hochoeppler, A., Kofod, P., and Zannoni, D. (1995) *FEBS Lett. 375*, 197−200.
20. Nunes, O. C., Donato, M. M., and da Costa, M. S. (1992) *System. Appl. Microbiol. 15*, 92−97.
21. Laemmli, U. K. (1970) *Nature 227*, 680−685.
22. Edman, P., and Begg, G. (1967) *Eur. J. Biochem. 1*, 80−90.
23. Layne, E. (1957) *Methods Enzymol. 3*, 447−454.
24. Fisher, D. S., and Price, D. C. (1964) *Clin. Chem. 10*, 21−25.
25. Teixeira, M., Batista, R., Campos, A. P., Gomes, C., Mendes, J., Pacheco, I., Anemüller, S., and Hagen, W. R. (1995) *Eur. J. Biochem. 227*, 322−327.
26. Anemüller, S., Bill, E., Schäfer, G., Trautwein, A. X., and Teixeira, M. (1992) *Eur. J. Biochem. 210*, 133−138.
27. Fieser, L. F. (1940) *J. Biol. Chem. 133*, 391−396.
28. Dawson, R. M. C., Elliott, D. C., Elliott, W. H., Jones, K. M. (1986) *Data for Biochemical Research*, 3rd ed., Oxford University Press, Oxford, England.
29. Morningstar, J. E., Johnson, M. K., Cecchini, G., Ackrell, B. A. C., and Kearney, E. B. (1985) *J. Biol. Chem. 260*, 13631−13638.
30. Maguire, J., Johnson, M. K., Morningstar, J. E., Ackrell, B. A. C., and Kearney, E. B. (1985) *J. Biol. Chem. 260*, 10909−10912.
31. Hederstedt, L., and Ohnishi, T. (1992) *Molecular mechanisms in Bioenergetics* (Ernster, L., Ed.) Chapter 7, pp 163−198, Elsevier, Amsterdam.
32. Werth, M. T., Cecchini, G., Manodori, A., Ackrell, B. A. C., Schröder, I., Gunsalus, R. P., and Johnson, M. K. (1990) *Proc. Natl. Acad. Sci. U.S.A. 87*, 8965−8969.
33. Wang, D., Meinhardt, S. W., Sackmann, U., Weiss, H., and Ohnishi, T. (1991) *Eur. J. Biochem. 197*, 257−264.
34. Leif, H., Sled, V. D., Ohnishi, T., Weiss, H., and Friedrich, T. (1995) *Eur. J. Biochem. 230*, 538−548.
35. Ambler, R. P., Meyer, T. E., and Kamen, M. D. (1993) *Arch. Biochem. Biophys. 306*, 215−222.
36. Van Driessche, G., Ciurli, S., Hochkoeppler, A., and Van Beeumen, J. J. (1997) *Eur. J. Biochem. 244*, 371−377.
37. Agarwal, A., Li, D., and Cowan, J. A. (1995) *Proc. Natl. Acad. Sci. U.S.A. 92*, 9440−9444.
38. Przysiecki, C. T., Meyer, T. E., and Cusanovich, M. A. (1985) *Biochemistry 24*, 2542−2549.
39. Banci, L., Bertini, I., Ciurli, S., Ferretti, S., Luchinat, L., and Piccioli, M. (1993) *Biochemistry 32*, 9387−9397.
40. Pennoyer, J. D., Ohnishi, T., and Trumpower, B. L. (1988) *Biochim. Biophys. Acta 935*, 195−207.
41. Anemüller, S., Hettmann, T., Moll, R., Teixeira, M., and Schäfer, G. (1995) *Eur. J. Biochem. 232*, 563−268.
42. Hägerhäll, C., Sled, V., Hederstedt, L., and Ohnishi, T. (1995) *Biochim. Biophys. Acta 1229*, 356−362.
43. Bennett, B., Gruer, M. J., Guest, J. R., and Thomsom, A. J. (1995) *Eur. J. Biochem. 233*, 317−326.
44. Kennedy, M. C., Mende-Mueller, L., Blodin, G. A., and Beinert, H. (1992) *Proc. Natl. Acad. Sci. U.S.A. 89*, 11730−11734.
45. Hofmeister, A. E. M., Albracht, S. P. J., and Buckel, W. (1994) *FEBS Lett. 351*, 416−418.
46. Cunningham, R. P., Asahara, H., and Bank, J. F. (1989) *Biochemistry 28*, 4450−4455.
47. Cecchin, G., Sices, H., Schröder, I., and Gunsalus, R. P. (1995) *J. Bacteriol. 177*, 4587−4592.
48. Tindall, B. J. (1991) *FEMS Microbiol. Lett. 80*, 65−68.
49. Lübben, M., Arnaud, S., Castresana, J., Warne, A., Albracht, S. P. J., and Saraste, M. (1994) *Eur. J. Biochem. 224*, 151−159.
50. Pereira, M. M., Carita, J. N., and Teixeira, M. (1999) *Biochemistry 38*, 1268−1275.

BI981807V